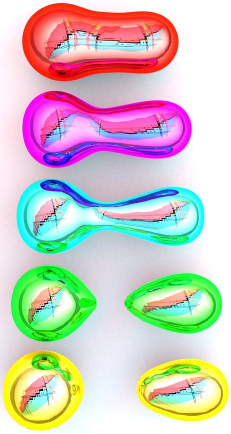

Sept. 09-13, 2019

Colloque GANIL

How the octupole structure determines the fission asymmetry

Guillaume SCAMPS

Collaboration : C. Simenel

Motivation : to understand the shell effects on fission

Empirical behaviour of actinide nuclei

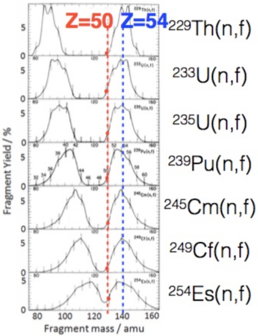

J.P. Unik, J.E. Gindler, J.E. Glendenin et al. : Proc. Phys. and Chem. of Fission IAEA Vienna , Vol II, 20 (1974)

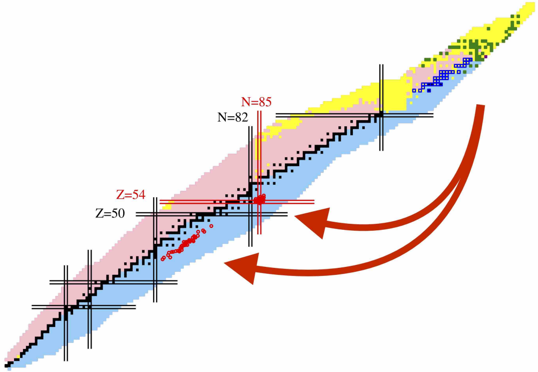

Data from D. A. Brown et al., Endf/b-viii.0, Nucl. Data Sheets 148, 1 (2018), (spontaneous and thermal neutron-capture).

Systematic comparison for actinide

Empirical behavior of actinide nuclei

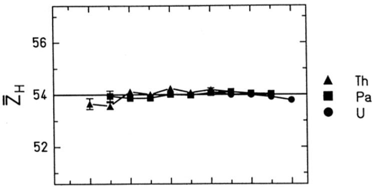

K.-H. Schmidt et al. Nuclear Physics A 665 (2000)

C. Böckstiegel et al. / Nuclear Physics A 802 (2008) 12–25

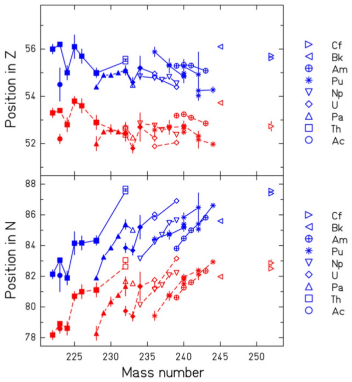

Motivation

How can we understand this behaviour ? Interplay between structure and reactions ?

Mean-field dynamics with pairing

TDHF+BCS

- Based on TDHFB with the approximation : $\Delta_{ij} = \delta_{ij}\Delta_i$
- Initialisation from ev8 (HF+BCS)
- Evolution : $i\hbar\frac{d\varphi_i}{dt} = (\hat{h}_{MF} - \epsilon_i)\varphi_i$

$$i\hbar\frac{dn_i}{dt} = \Delta_i^*\kappa_i - \Delta_i\kappa_i^*$$

$$i\hbar\frac{d\kappa_i}{dt} = \kappa_i(\epsilon_i - \epsilon_{\bar{i}}) + \Delta_i(2n_i - 1)$$

Details of the calculation

- Skyrme functionnal Sly4d
- Surface pairing interaction
- $\Delta x = 0.8$ fm ; $\Delta t = 1.5 \times 10^{-24}$ s
- Lattice : $L_x \times L_y \times 2L_z = 40 \times 19.2 \times 19.2$ fm^3

Why does we need pairing ?

Fission barrier : ^{258}Fm

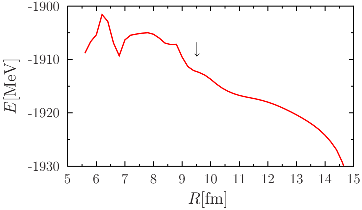

TDHF

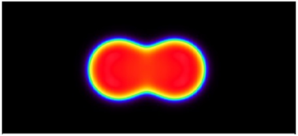

TDHF+BCS

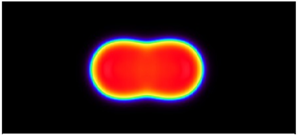

G. Scamps, C. Simenel, D. Lacroix, PRC **92**, 011602(R) (2015).

Why does we need pairing ?

Fission barrier : ^{258}Fm

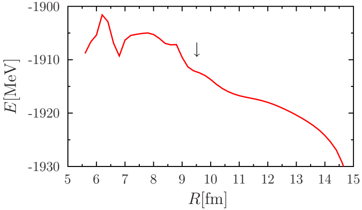

TDHF

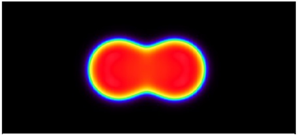

TDHF+BCS

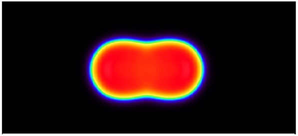

G. Scamps, C. Simenel, D. Lacroix, PRC **92**, 011602(R) (2015).

Why does we need pairing ?

Fission barrier : ^{258}Fm

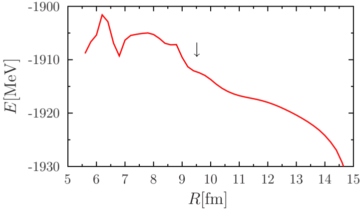

TDHF

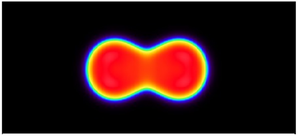

TDHF+BCS

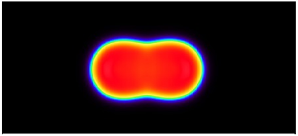

G. Scamps, C. Simenel, D. Lacroix, PRC **92**, 011602(R) (2015).

Influence of pairing on fission process

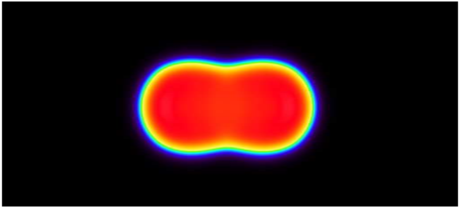

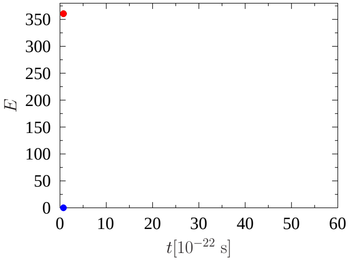

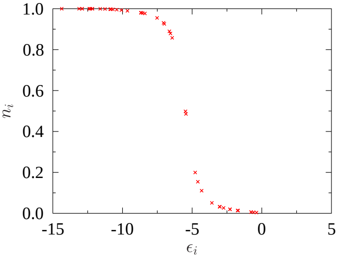

Influence of pairing on fission process

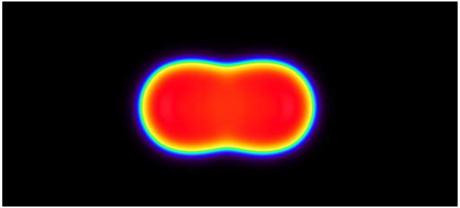

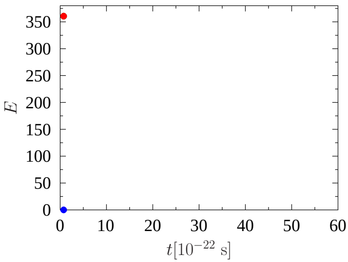

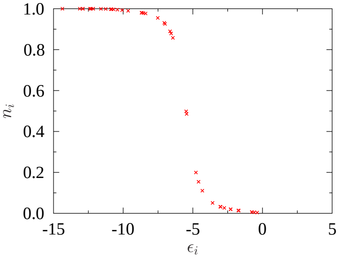

New systematic study

First : CHF+BCS

Example : ^{240}Pu

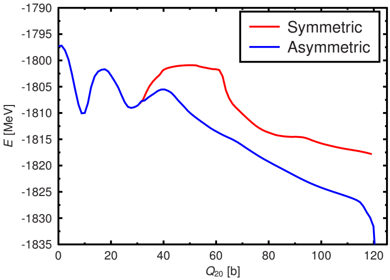

Second : TDHF+BCS

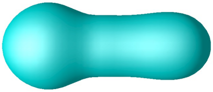

New systematic study

First : CHF+BCS

Example : ^{240}Pu

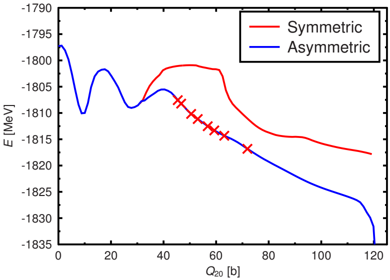

Second : TDHF+BCS

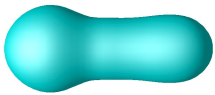

New systematic study

First : CHF+BCS

Example : ^{240}Pu

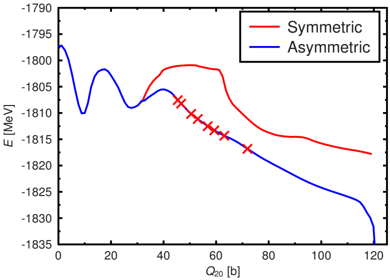

Second : TDHF+BCS

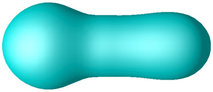

TDHF+BCS systematics results

TDHF+BCS

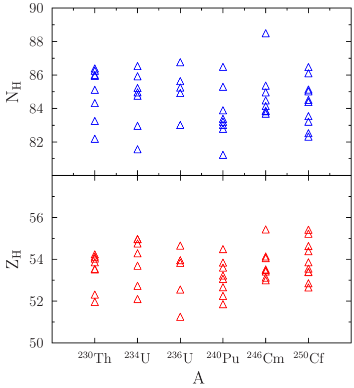

Comparison with experimental data

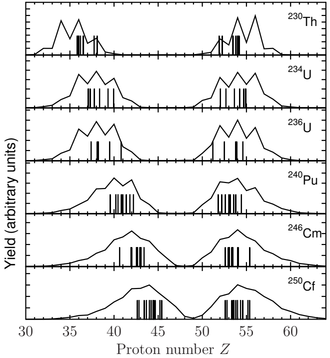

TDHF+BCS systematics results

TDHF+BCS

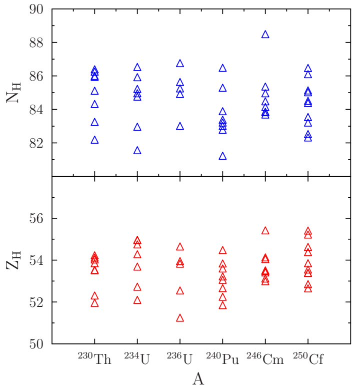

Comparison with experimental data

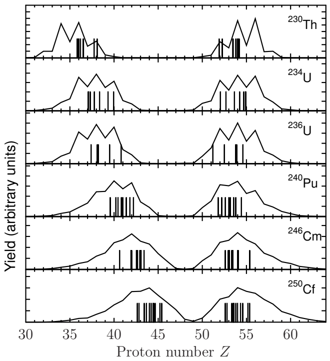

Conclusion :

The TDHF+BCS calculation reproduces well the Z=54 behavior. But why ?

Nucleon localization function

Fermion localization function

$$\mathcal{C}_{q\sigma}(\mathbf{r}) = \left[1 + \left(\frac{\tau_{q\sigma}\rho_{q\sigma} - \frac{1}{4}|\nabla\rho_{q\sigma}|^2 - \mathbf{j}_{q\sigma}^2}{\rho_{q\sigma}\tau_{q\sigma}^{TF}} \right)^2 \right]^{-1}$$

A. D. Becke and K. E. Edgecombe, J. Chem. Phys. 92, 5397 (1990).

Physical meaning :
$\mathcal{C} \in [0:1]$
$\mathcal{C}_{q\sigma}(\mathbf{r}) = 1$ Probability to find another particle with the same q and σ very low.
$\mathcal{C}_{q\sigma}(\mathbf{r}) = 0.5$ Limit of uniform-density Fermi gas.

Mask function :

$$\rightarrow \frac{\mathcal{C}_{q\sigma}(\mathbf{r})\rho_{q\sigma}}{\rho_{q\sigma}^{\max}}$$

Nucleon localization function

Fermion localization function

$$\mathcal{C}_{q\sigma}(\mathbf{r}) = \left[1 + \left(\frac{\tau_{q\sigma}\rho_{q\sigma} - \frac{1}{4}|\nabla\rho_{q\sigma}|^2 - \mathbf{j}_{q\sigma}^2}{\rho_{q\sigma}\tau_{q\sigma}^{TF}}\right)^2\right]^{-1}$$

A. D. Becke and K. E. Edgecombe, J. Chem. Phys. 92, 5397 (1990).

Physical meaning :
$\mathcal{C} \in [0:1]$
$\mathcal{C}_{q\sigma}(\mathbf{r}) = 1$ Probability to find another particle with the same q and σ very low.
$\mathcal{C}_{q\sigma}(\mathbf{r}) = 0.5$ Limit of uniform-density Fermi gas.

Mask function :

$$\rightarrow \frac{\mathcal{C}_{q\sigma}(\mathbf{r})\rho_{q\sigma}}{\rho_{q\sigma}^{\max}}$$

Example :

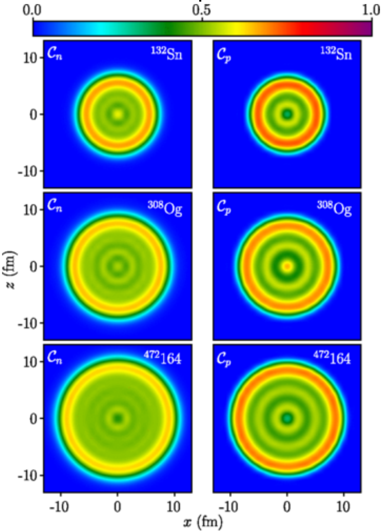

P. Jerabek, B. Schuetrumpf, P. Schwerdtfeger, and W. Nazarewicz, Phys. Rev. Lett. **120**, 053001 (2018).

Nucleon localization function

Fermion localization function

$$\mathcal{C}_{q\sigma}(\mathbf{r}) = \left[1 + \left(\frac{\tau_{q\sigma}\rho_{q\sigma} - \frac{1}{4}|\nabla\rho_{q\sigma}|^2 - \mathbf{j}^2_{q\sigma}}{\rho_{q\sigma}\tau^{TF}_{q\sigma}}\right)^2\right]^{-1}$$

A. D. Becke and K. E. Edgecombe, J. Chem. Phys. 92, 5397 (1990).

Physical meaning :
$\mathcal{C} \in [0:1]$
$\mathcal{C}_{q\sigma}(\mathbf{r}) = 1$ Probability to find another particle with the same q and σ very low.
$\mathcal{C}_{q\sigma}(\mathbf{r}) = 0.5$ Limit of uniform-density Fermi gas.

Mask function :

$$\rightarrow \frac{\mathcal{C}_{q\sigma}(\mathbf{r})\rho_{q\sigma}}{\rho^{\max}_{q\sigma}}$$

Schematic system

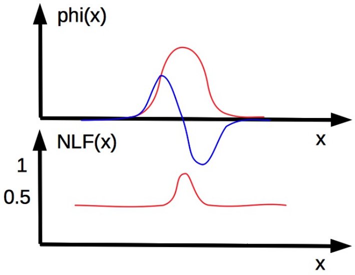

Example of ^{240}Pu

^{240}Pu

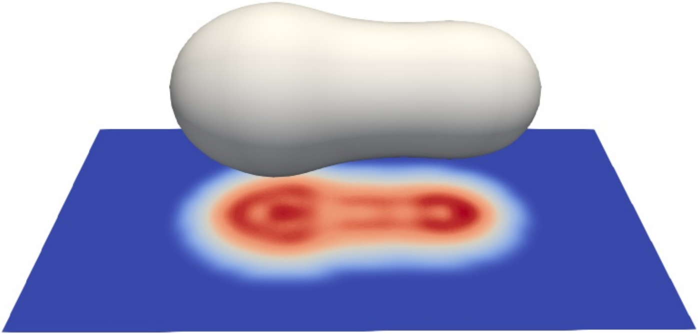

Example of ^{240}Pu

^{240}Pu

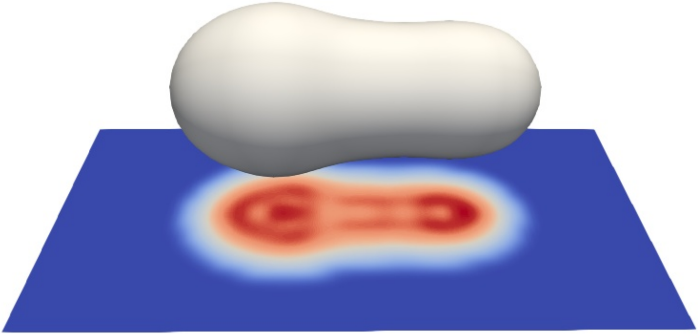

Example of ^{240}Pu

^{240}Pu

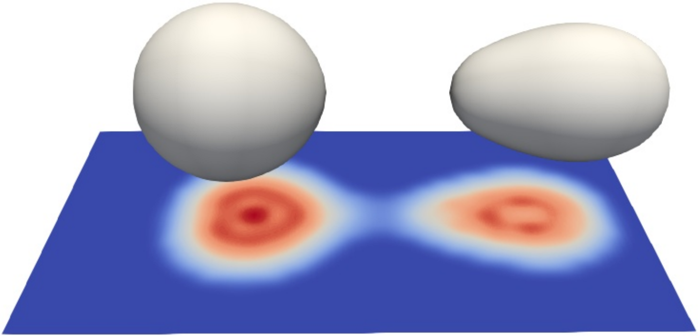

Example of ^{240}Pu

^{240}Pu

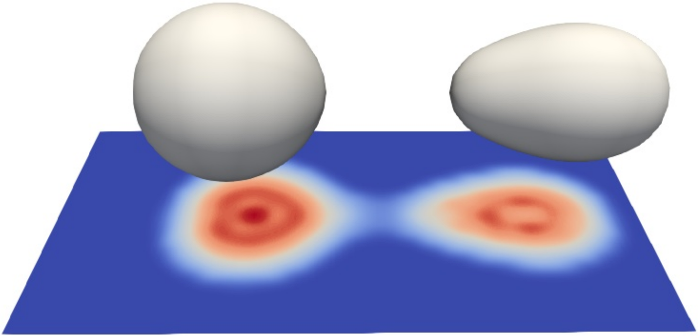

Example of ^{240}Pu

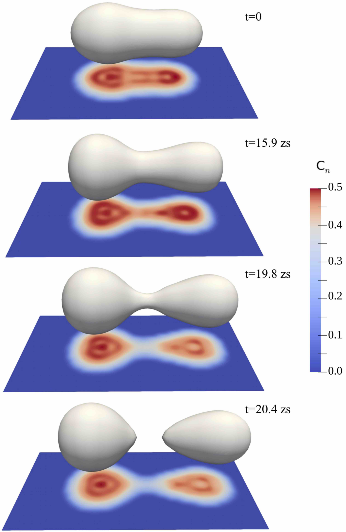

Hypothesis

The octupole shell effects are important in the fission fragment

Other systems

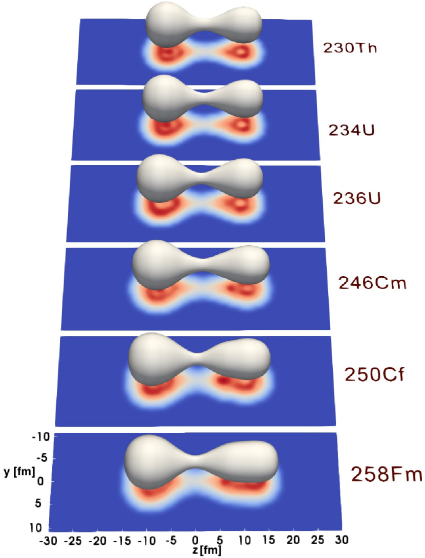

Other systems

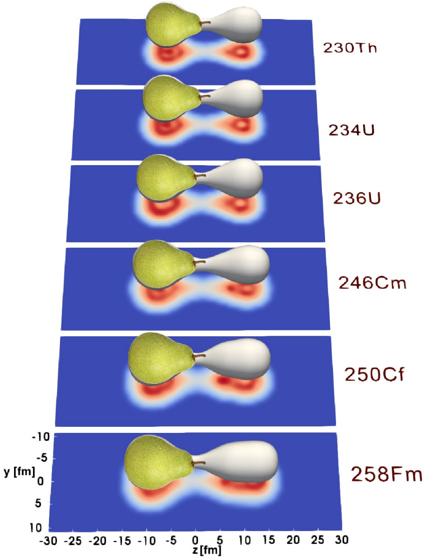

Why the fragments have octupole deformation ?

Similar effect on fusion reaction

^{40}Ca+^{40}Ca, $E3^{-} = 3.7$ MeV

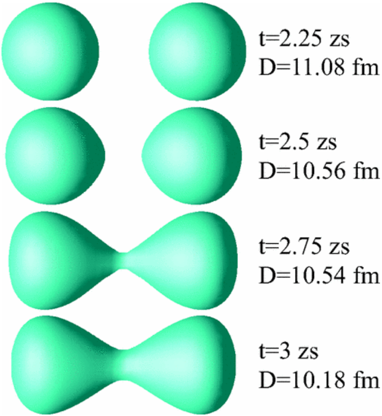

^{56}Ni+^{56}Ni, $E3^{-} = 7.5$ MeV

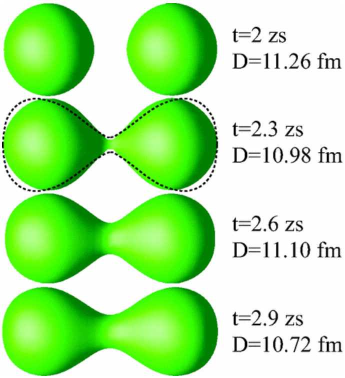

C. Simenel, M. Dasgupta, D. J. Hinde, and E. Williams, Phys. Rev. C 88, 064604 (2013).

Why the fragments have octupole deformation ?

Similar effect on fusion reaction

^{40}Ca+^{40}Ca, $E3^{-} = 3.7$ MeV

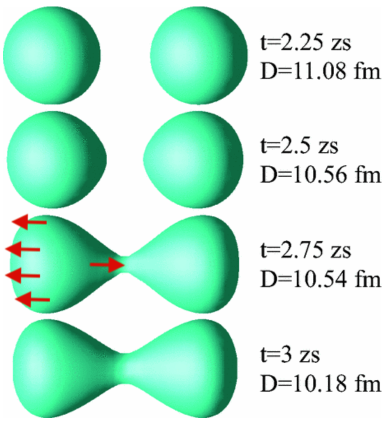

^{56}Ni+^{56}Ni, $E3^{-} = 7.5$ MeV

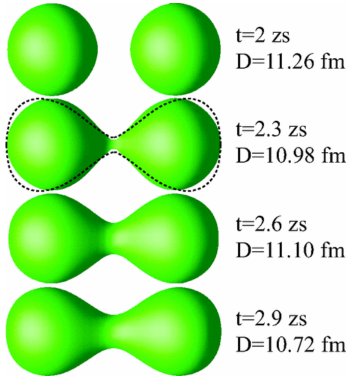

C. Simenel, M. Dasgupta, D. J. Hinde, and E. Williams, Phys. Rev. C 88, 064604 (2013).

Octupole deformation systematics

Skyrme Skm*.

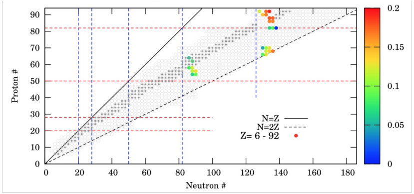

S. Ebata, and T. Nakatsukasa, Phys. Scr. 92 (2017) 064005

Gogny D1S

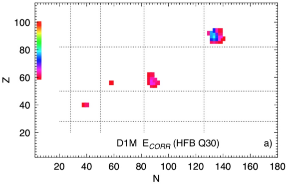

LM Robledo - J. phys. G : Nucl. and Particle Physics, 2015

Results from systematic calculation

In both calculations, the region $Z \simeq 56$, $N \simeq 88$ is favorable for octupole deformation .

Experimental results

^{144}Ba is found to be octupole in its groud state. Burcher et al. PRL 116 (2016).

Octupole deformation systematics

Skyrme Skm*.

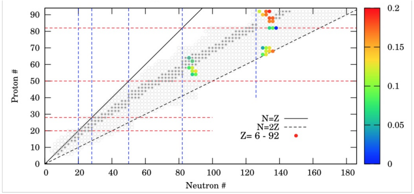

S. Ebata, and T. Nakatsukasa, Phys. Scr. 92 (2017) 064005

Fission data

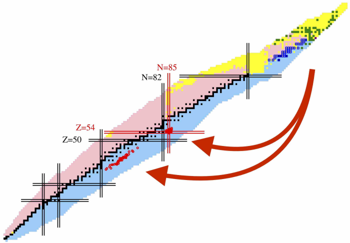

Results from systematic calculation

In both calculations, the region Z $\simeq$ 56 , N $\simeq$ 88 is favorable for octupole deformation .

Experimental results

^{144}Ba is found to be octupole in its groud state. Burcher et al. PRL 116 (2016).

Constraint HF+BCS octupole deformation with Sly4d

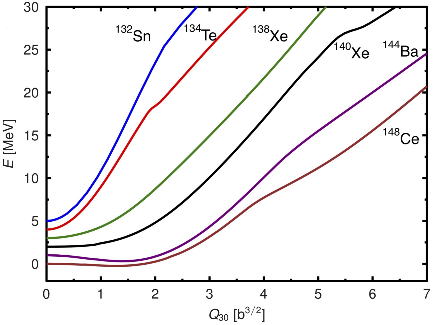

Result from constraint calculation of the heavy fragment

The gain in energy due to the octupole softness drives the fission to the $Z \simeq 54$

Structure, ^{144}Ba, Z=56, N=88

Q_2 - Q_3 potential energy surface

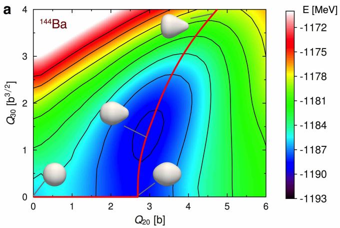

Single particle energy

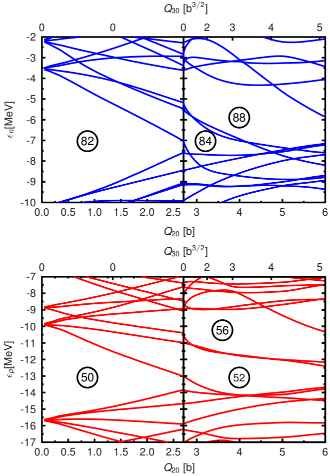

Structure

Single particle energies

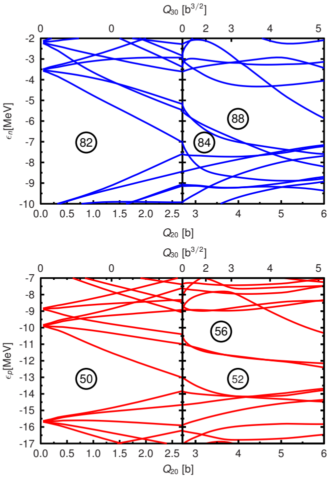

Experimental results

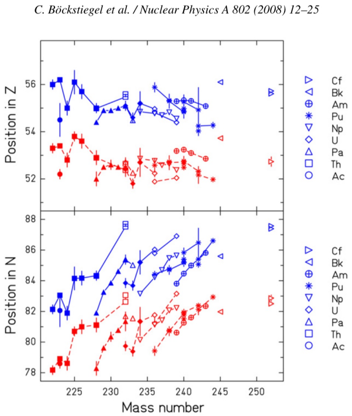

Structure

Single particle energies

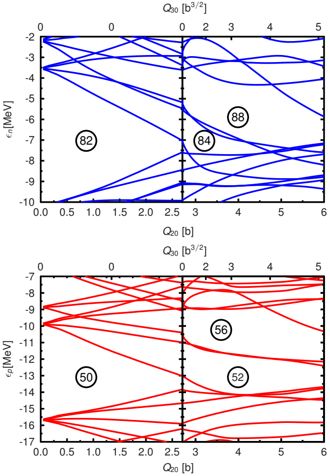

Experimental results

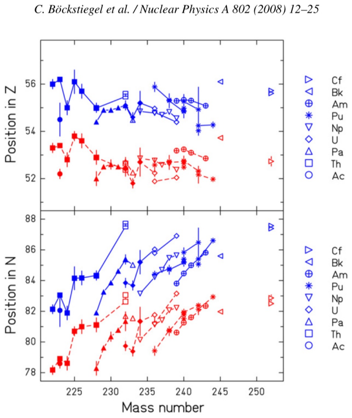

We need Z and N identification pre-evaporation → VAMOS at GANIL (see next talk by Diego Ramos).

Deformation energy at the scission. Simple scission point model

$$E(N,Z) = E_{\beta_3=0.35}(N,Z) + E_{\beta_2=0.8}(N_{\rm tot}-N, Z_{\rm tot}-Z) + e^2\frac{Z(Z_{\rm tot}-Z)}{D_{sc}}$$

With D_{sc}=17 fm. On the map, $E(N,Z) - E_{min}$ is shown.
For ^{240}Pu, $N_{\rm tot}$=146 and $Z_{\rm tot}$=94

Octupole deformation

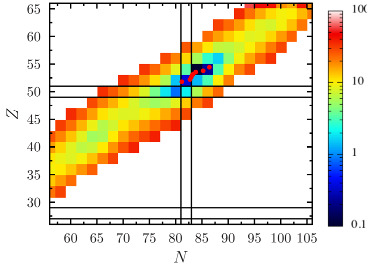

Spherical heavy fragment

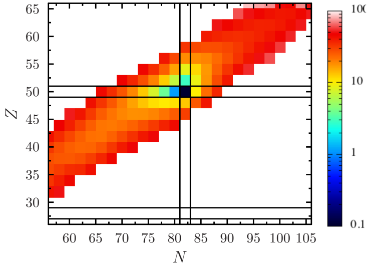

The energies have been calculated with the CHF+BCS theory Sly4d

Identification method with the nucleon localisation function

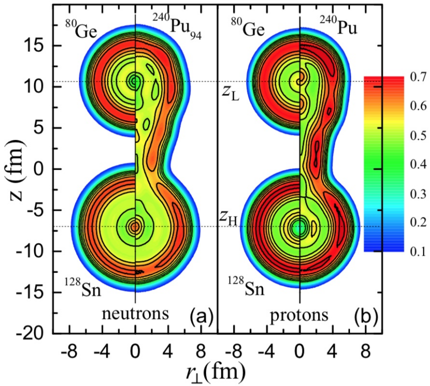

This method assumes that the pre-fragments have reflexion symmetry.
J. Sadhukhan, C. Zhang, W. Nazarewicz, and N. Schunck, PRC 96, 061301(R) (2017).

Identification with density

Technique of : M. Warda, A. Staszczak, and W. Nazarewicz, PRC 86, 024601 (2012).

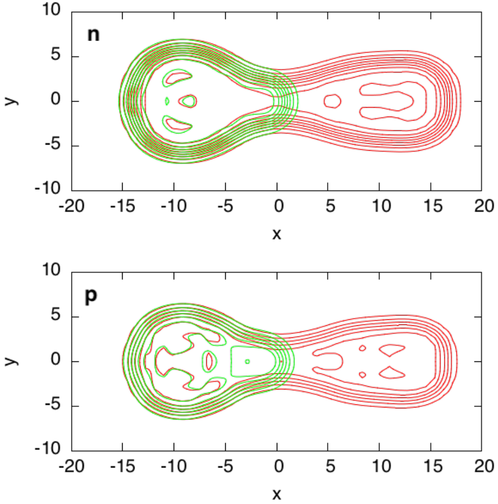

Green contour line : density of a ^{144}Ba with a constraint β_3=0.42
Red contour line : density of a fissioning ^{258}Fm (asymmetric mode)

Identification with nucleon localisation function

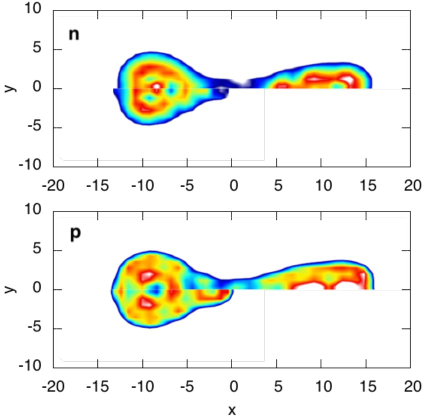

Top : NLF of a ^{144}Ba with a constraint β_3=0.42
Bottom : NLF of a fissioning ^{258}Fm (asymmetric mode)

Identification with nucleon localisation function

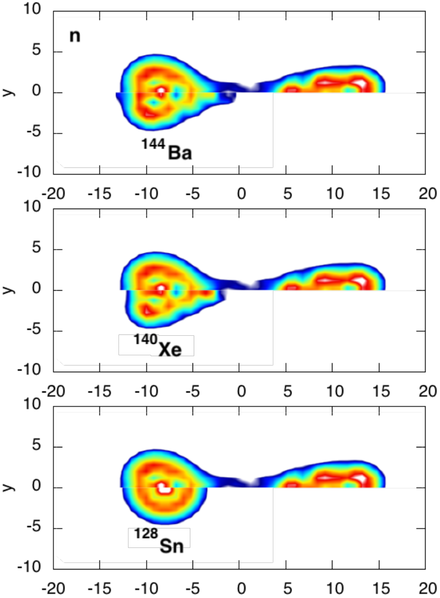

Identification method with octupole degree of freedom

Identification of the fragments as a function of time for the fission of ^{258}Fm

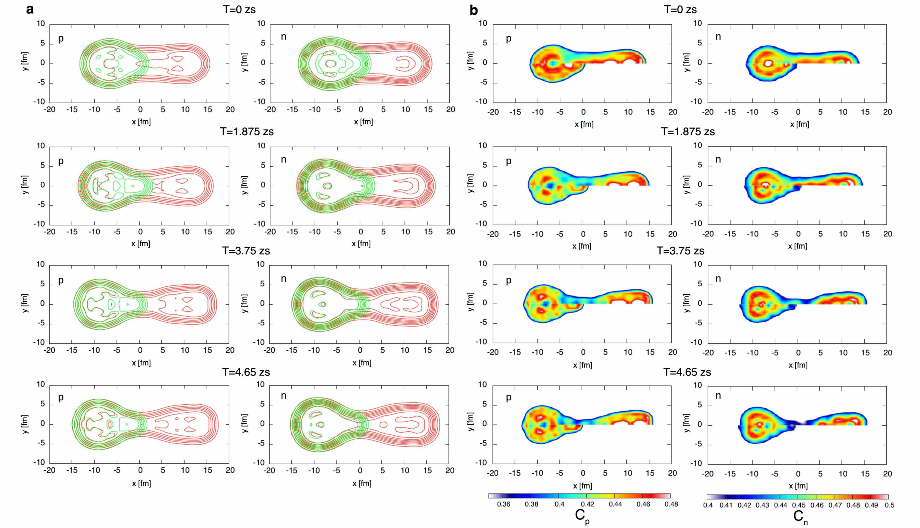

All of the systems are identified as ^{144}Ba with different β_3 values (resp. 0.14, 0.39, 0.39 and 0.42)

Identification method with octupole degree of freedom

Identification of the fragments at the scission for the different elements.

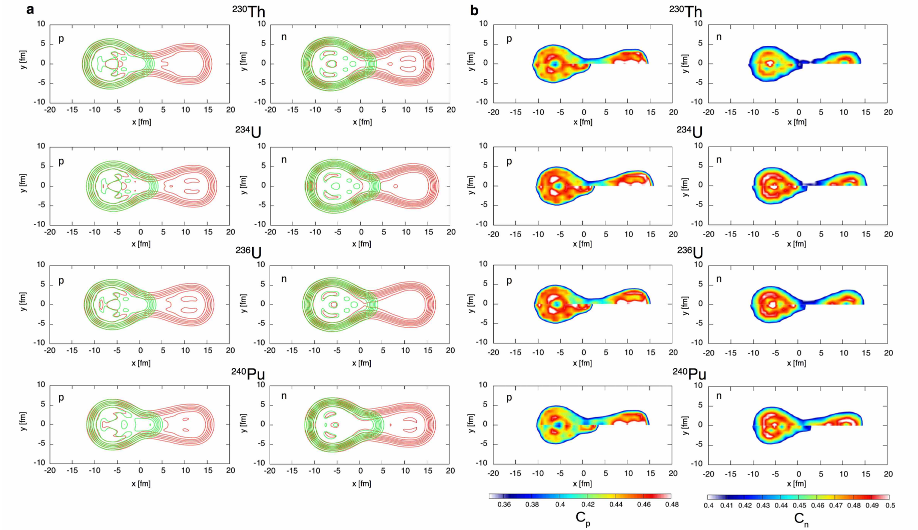

All systems are identified as ^{144}Ba with different β_3 values (resp. 0.28, 0.28, 0.27 and 0.44)

Conclusion

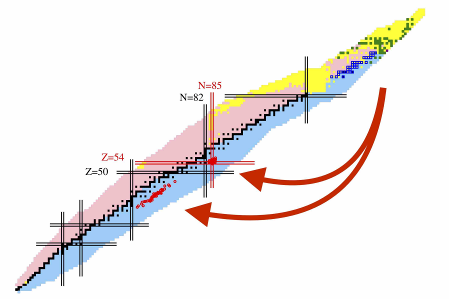

Mechanism

- The Nucleus-Nucleus interaction at the scission configuration favors the octupole shapes
- Shell structure favors octupole shape in the region $Z \simeq 52\text{-}56$, $N \simeq 84\text{-}88$
- Actinide fission fragments are driven in the region $Z \simeq 54$, $N \simeq 86$

G. Scamps, C. Simenel, Nature 564, 382 (2018).

Similar effect for other systems ?

P. A. Butler.

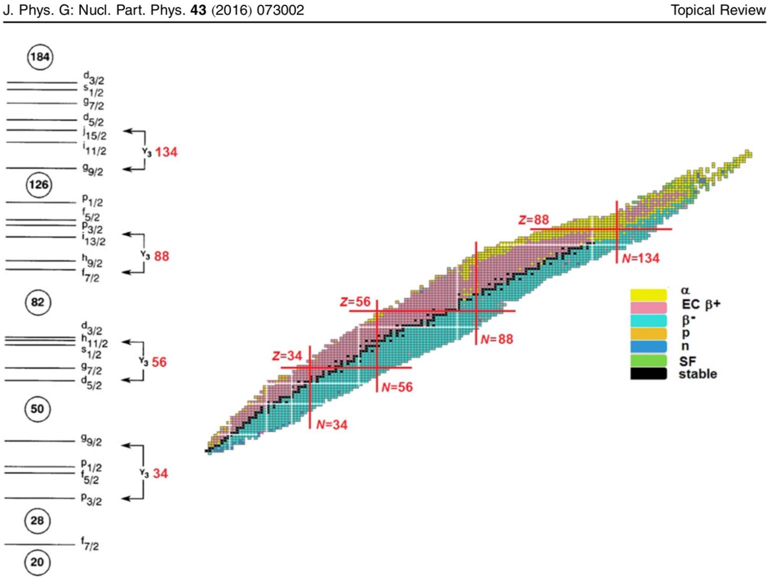

Experimental data of ^{180}Hg

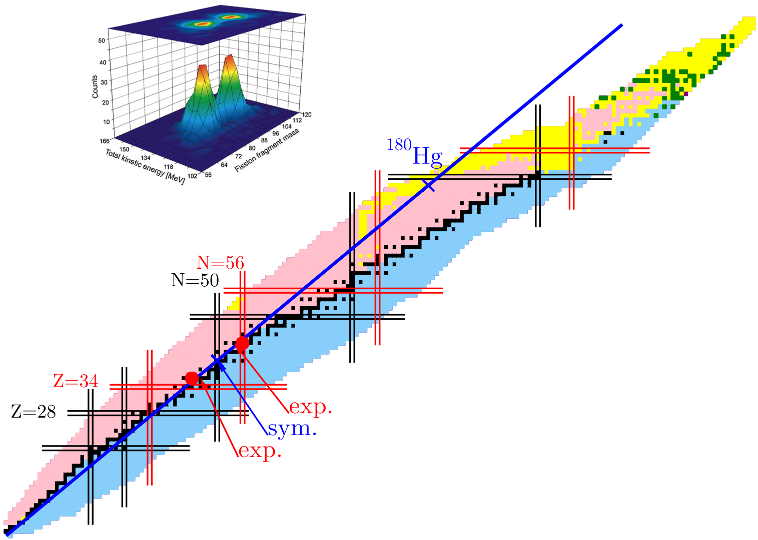

Experimental data of ^{178}Pt

I. Tsekhanovich, et al. PLB 790 (2019).

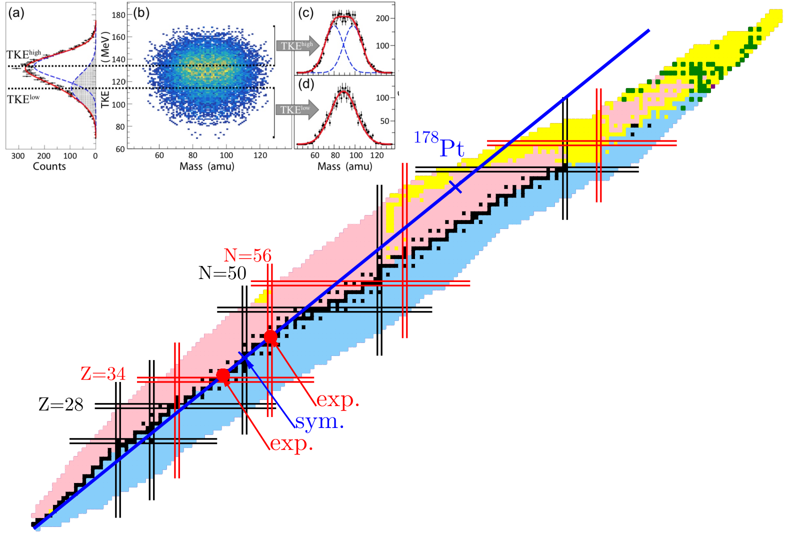

Similar effect of the octupole deformation ?

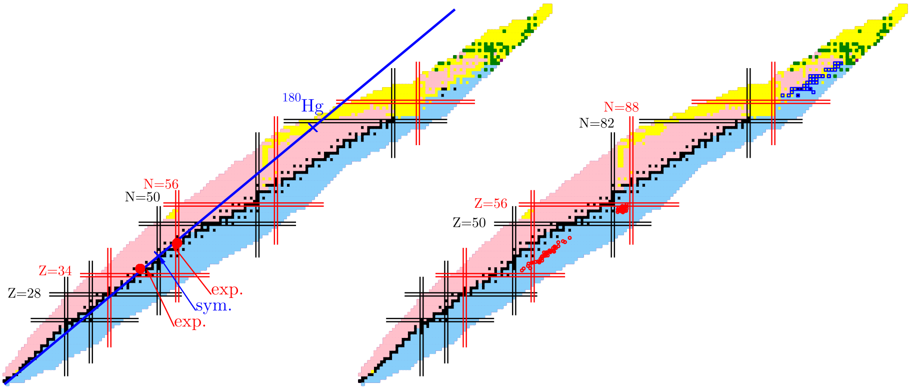

CHF+BCS calculation

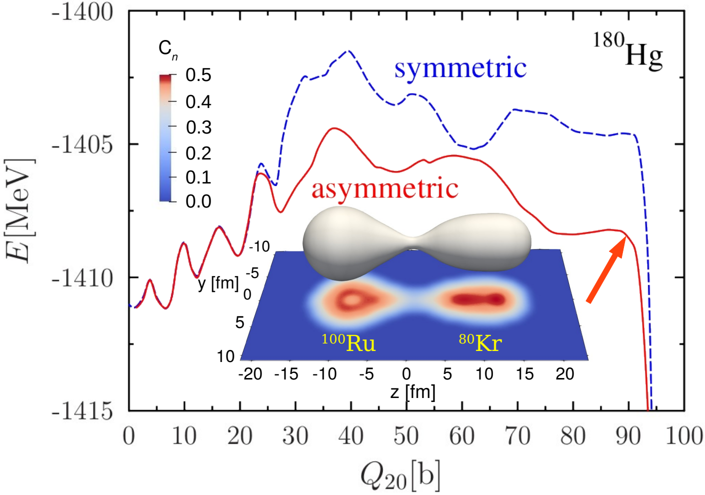

Comparison with experimental data

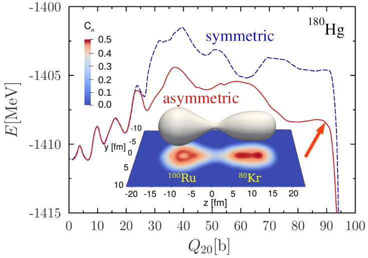

Experimental article : A. N. Andreyev, et al. Phys. Rev. Lett. 105, 252502 (2010).

and the fission-fragment mass is shown in Fig. 4. The mass distribution is clearly asymmetric, with the most probable heavy and light masses of $A_H = 100(1)$ and $A_L = 80(1)$, having a width of sigma = 4.0(3) amu. The most probable

Z values of the heavy and light fission fragments are deduced to be $Z_H = 44(2)$ and $Z_L = 36(2)$, respectively, assuming that the N/Z ratio of the parent nucleus ^{180}Hg is preserved in the fission fragments. Thus, the most abundantly produced fission fragments are ^{100}Ru and ^{80}Kr and their neighbors. Although 75% of the fission events are

Single-particle energies in the heavy fragment

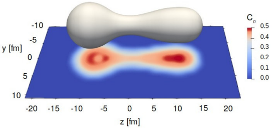

Structure of ^{100}Ru (Z=44 and N=56)

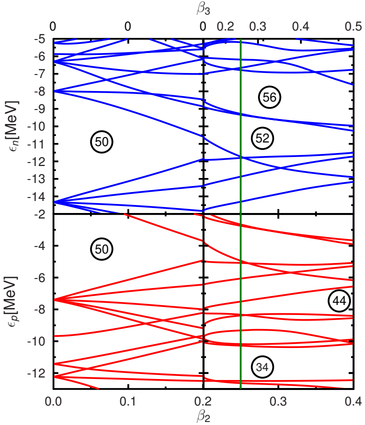

Single-particle energies in light fragment. New method.

Structure of pre-fragment (Z=34 and N=44)

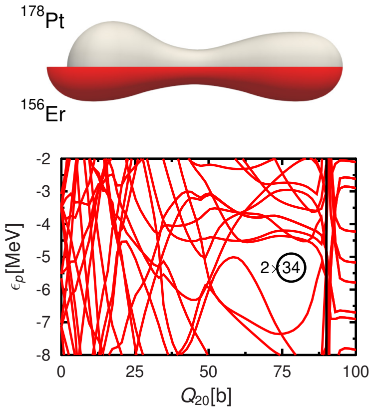

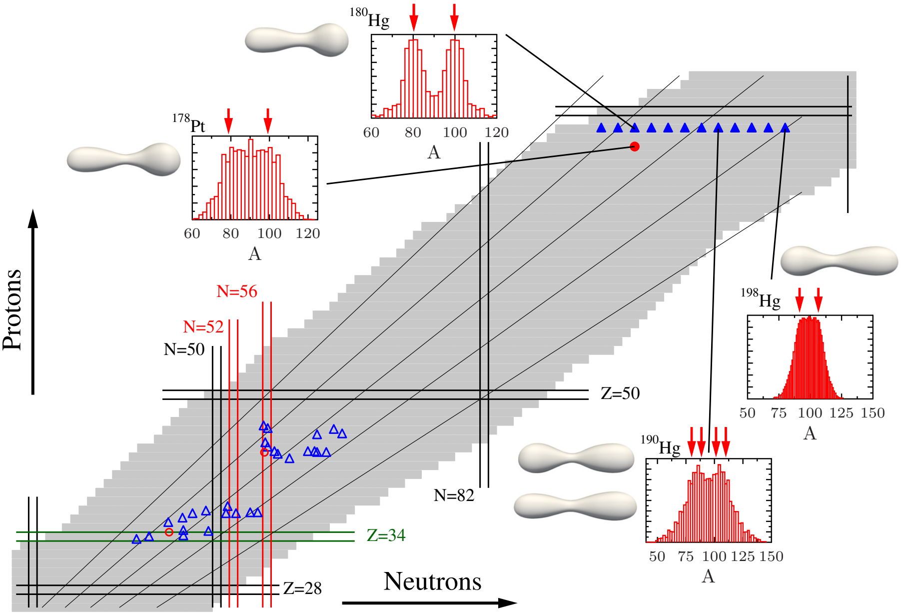

G. Scamps and C. Simenel, arXiv :1904.01275

CHF+BCS calculations : Hg isotopic chain

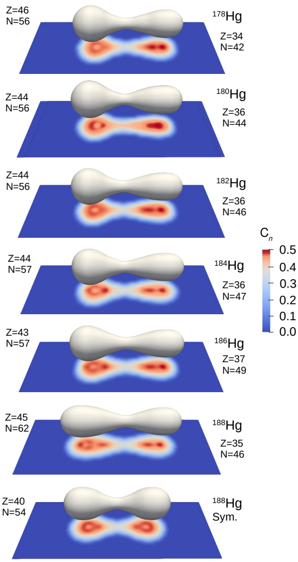

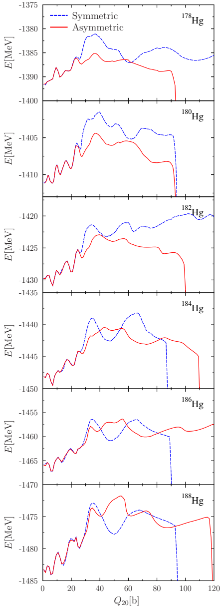

Conclusion

The fission process magnifies the octupole shell structure

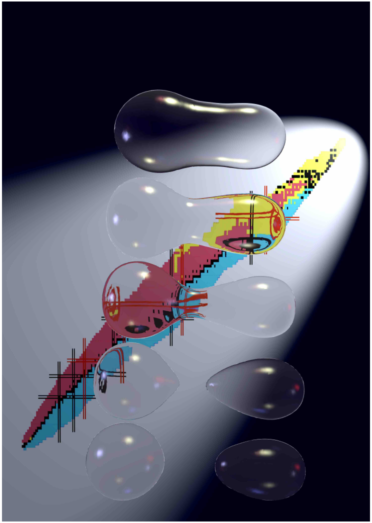

Thank you

Comparison TDHFB - TDHF+BCS

TDHFB

- Quasi-particles : $|\omega_\alpha\rangle = \binom{U_\alpha}{V_\alpha}$
- Evolution : $i\hbar \frac{d|\omega_\alpha\rangle}{dt} = \begin{pmatrix} h & \Delta \\ -\Delta^* & -h^* \end{pmatrix} |\omega_\alpha\rangle$

TDHF+BCS

- Based on TDHFB with the approximation : $\Delta_{ij} = \delta_{ij}\Delta_i$
- Evolution : $i\hbar \frac{d\varphi_i}{dt} = (\hat{h}_{MF} - \epsilon_i)\varphi_i$

$$i\hbar \frac{dn_i}{dt} = \Delta_i^* \kappa_i - \Delta_i \kappa_i^*$$

$$i\hbar \frac{d\kappa_i}{dt} = \kappa_i(\epsilon_i - \epsilon_{\bar{i}}) + \Delta_i(2n_i - 1)$$

Theoretical difference

- Numerical cost : TDHFB requires 1000 times more numerical resources
- Treatment of continuum states : BCS gas problem
- Continuity equation
- Number of pairing degrees of freedom (HFB $\Delta(r)$, BCS : $\Delta_{i\bar{i}}$)
- Spatial dependence of the pairing correlation

Comparison for fission of ^{240}Pu

A. Bulgac, P. Magierski, K. J. Roche, and I. Stetcu, PRL 116, 122504 (2016).

S no.	η	E^*	E_n	q_{zz}	q_{zzz}	t_{SS}	TKE^{syst}	TKE	A_L^{syst}	A_L	N_L^{syst}	N_L	Z_L^{syst}	Z_L
$S1$	0.75	8.05	1.52	1.78	−0.742	14 419	177.27	182	100.55	104.0	61.10	62.8	39.45	41.2
$S2$	0.5	7.91	1.38	1.78	−0.737	4360	177.32	183	100.56	106.3	60.78	64.0	39.78	42.3
$S3$	0	8.08	1.55	1.78	−0.737	14 010	177.26	180	100.55	105.5	60.69	63.6	39.81	41.9
$S4$	0	6.17	−0.36	2.05	−0.956	12 751	177.92	181		103.9		62.6		41.3

TABLE – TDHF+BCS results for ^{240}Pu

#	Q_0 [b]	E_0^*[MeV]	T_{fis} [fm/c]	Z_L	N_L	TKE [MeV]
1	45.4	1.46	6480	40.21	60.77	171.5
2	46.7	0.8	4830	40.83	62.68	181.8
3	50.5	-1.16	26970	42.2	64.83	181.8
4	53.0	-2.13	6750	41.39	63.05	177.9
5	56.8	-3.5	4800	40.99	62.85	177.2
6	59.3	-4.3	5400	40.45	62.17	178.4
7	63.1	-5.31	6630	39.55	59.58	162.7
8	71.9	-7.8	1020	41.8	63.28	179.9